P1R.15 **A Suite of Retrieval Algorithms for Cirrus Cloud Microphysical Properties Applied To Lidar, Radar, and Radiometer Data Prepared for the A-Train**

Yuying Zhang * and Gerald G. Mace
Department of Meteorology, University of Utah

1. Introduction

CloudSat and CALIPSO (Stephens et al., 2002) will fly in formation with Aqua and the footprints of the three spacecraft will overlap each other within several minutes. Observational data from the A-Train satellite constellation will provide a unique opportunity to derive a global description of the occurrence and properties of cirrus clouds. CloudSat will fly the first spaceborne millimeter wavelength radar. The Cloud Profiling Radar (CPR) on CloudSat will operate at the microwave frequency of 94 GHz (~3mm wavelength) with a sensitivity defined by a minimum detectable reflectivity factor of -28 dBZe. The CPR will have a footprint of 1.4 km across by 2.5 km along track, and 500m vertical resolution that will be oversampled to provide 250m range gates. Based on the advantages of the different remote-sensing techniques, the multi-sensor cloud properties are retrieved to characterize cirrus clouds.

In this paper, the forward model equations are described to convert the data streams from the individual multiple remote sensors into layer-averaged cirrus bulk microphysical properties in section 2. The sensitivity of three potential algorithms to the input and empirical constants is analyzed in section 3. In section 4, the algorithms are implemented on data collected during CRYSTAL-FACE, and further evaluation of the current algorithms are performed using observations from MODIS on Terra combined with MMCR and MPL data collected at the ARM SGP site.

2. Algorithm Description

In order to retrieve cloud properties, the layer-mean ice crystal size spectrum is assumed in the form of a two-parameter exponential function $n(L)=N_e exp(-\lambda_e L)$ where N_e is the intercept with units of number per unit length per unit volume of particles and λ_e is the logarithmic slope of the size spectrum and has units of inverse length. Since ice crystals are not solid spheres of diameter *L*, the forward model must include a set of empirical expressions that relate the maximum dimension of an ice crystal with the particle cross sectional area (*A*(*L*)), radar backscatter cross section, and particle mass (*m*(*L*)). It is a conventional approach to express these relations in a power-law form where the coefficients depend on crystal habit (Mitchell 1996; Aydin and Walsh 1999; Heymsfield and Iaquinta 2000; Heymsfield et al. 2002).

A MODIS CO_2 channel (band 34/35) (Wylie and Menzel, 1989; Wylie et al., 1994) is used to convert infrared radiance to cloud layer emissivity (Liou, 2002; Wylie and Menzel, 1989; Wylie et al., 1994):

$$N\varepsilon = \frac{R(\lambda) - R_{clr}(\lambda)}{B[\lambda, T(P_c)] - R_{clr}(\lambda)} \quad (1)$$

Nε is the effective cloud amount observed in the window band referring to the product of the fractional cloud cover N and the cloud emissivity ε for each observational area. *R(λ)* is the cloudy infrared radiance observed at the satellite, *Rclr(λ)* is the clear-sky infrared radiance calculated from atmospheric temperature and pressure profile, and *B[λ,T(p)]* is the Planck function for band λ and temperature *T* at pressure level *P.* The infrared absorption coefficient:

$$\beta_a = \int_0^\infty Q_a(L)A(L)n(L)dL \quad (2)$$

is derived from layer emissivity ($\varepsilon = 1 - \exp[-\beta_a \Delta h]$). Data for the absorption efficiency, Q_a, as a function of ice particle size in the CO_2 channel (13-14 μm) is calculated by Dr. Ping Yang of Texas A&M University based on a composite method using T_matrix, Geometric Optics Method (GOM), and Mie theory (Yang et al., 2004).

The visible extinction coefficient in the lidar wavelengths:

$$\beta_{ext} = \int_0^\infty Q_{ext} \cdot A(L)n(L)dL \quad (3)$$

as derived from cloud transmissivity ($T = \exp(-\tau)$, $\tau = \int_0^\infty \beta_{ext} \cdot dh$)assumes Q_{ext} to be a constant 2 since the particles are on the order of tens to hundreds of microns whereas the lidar wavelengths are in the 0.5 μm range. Radar reflectivity factor *Ze* is expressed as

$$Z_e = a_z \int_0^\infty n(L)L^{6+b_z}dL \cdot \quad (4)$$

The basic microphysical properties of cirrus clouds that we wish to derive from the observations are the ice water content (*IWC*) and mass-mean length (L_{mass}):

$$IWC = \int_0^\infty m(L)n(L)dL \quad (5)$$

$$L_{mass} = \int_0^\infty Lm(L)n(L)dL / \int_0^\infty m(L)n(L)dL \quad (6)$$

Radar-Lidar algorithm is hereafter referred to as the ZS algorithm, the Radar-Radiometer algorithm is referred to as the ZR algorithm, and the Radiometer-Lidar algorithm is referred to as the RS algorithm.

3. Sensitivity Study

The response of the retrieval algorithm to typical values of the observations is shown in Figure 1, 2 and 3. Figure 1 is calculated from the Z-R algorithm, and Figure 2 is calculated from the Z-S algorithm. The retrieved parameters depend to a nearly equal degree on the input parameters, and the retrieval results tend to remain within the ranges typical of cirrus (Dowling and Radke 1990; Mace et al. 2001). For a given radar

* Corresponding author address: Yuying Zhang, Dept. Meteorology, Univ. of Utah, SLC UT 84112-0110; Email: zyuying@met.utah.edu

reflectivity, the water content increases for increasing beam emittance, and the water content decreases for increasing beam transmittance. Holding the beam emittance or the transmittance constant, the water content increases with increasing radar reflectivity. For the R-S algorithm, the information to solve the system of equations for *IWC* comes from the different dependencies of infrared Q_a and visible Q_e on the characteristics of the particle size distribution. Small changes in one observation relative to the other will cause a large change in the retrieved values. We can expect this algorithm to be the most unstable algorithm of the three considered.

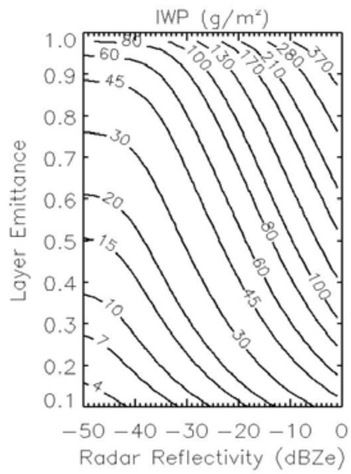

Figure 1. IWP response of the ZR algorithm to typical values of layer emittance and radar reflectivity. The assumed cloud depth is 2 km.

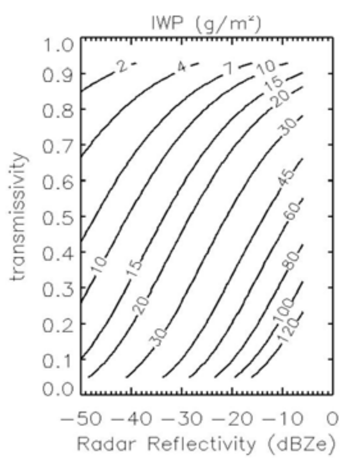

Figure 2. IWP response of the ZS algorithm to typical values of layer transmittance and radar reflectivity. The assumed cloud depth is 2 km.

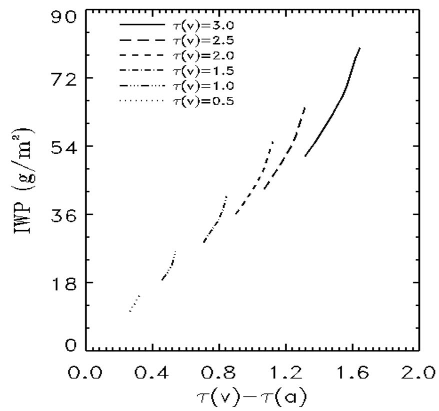

Figure 3. The IWP (assuming 2 km cirrus cloud) as a function of the difference/fractional difference between the visible τ_v and the infrared τ_a.

The retrieved properties are sensitive to the empirical constants assumed in all the algorithms. For example, in the Z-R algorithm, when a_m decreases and increases 50 percent, *IWC* changes linearly, but the change is very nonlinear with a_a and a_z. *IWC* is also quite sensitive to the specified values of b_m, b_a and b_z. This analysis shows that large uncertainties in the retrievals arise due to small uncertainties in the empirical constants. For the purpose of processing global data from the A-Train, empirical constants should ideally be derived based on extensive in-situ aircraft data that spans various heights and geographical locations where ice crystal area, size, and condensed mass are measured independently. Since such a database is not yet available, we utilize the existing data for this purpose and properly account for the associated uncertainties in the inversion formalism.

4. Implementation and Evaluation

On 26 July 2002 during the CRYSTAL-FACE mission, the ER-2 flew southward into the tropics eventually paralleling the eastern Yucatan coast, and returned along the same track. We examine a portion of that flight from 18:06:00 to 19:12:00 UTC hours. The extensive cirrus field that was observed along this flight track may be representative of much of the tropical cirrus that will be observed by the A-Train. Figure 4 shows the lidar signal, radar reflectivity, MAS brightness temperature in a band similar to the MODIS channel 34, and retrieved layer-mean *IWC* for the southbound leg in (a) and northbound leg in (b). Much of the cirrus is well below the detection threshold (~ -28 *dBZ*) of the ER2 Cloud Radar System (CRS; data provided courtesy of G. Heymsfield).

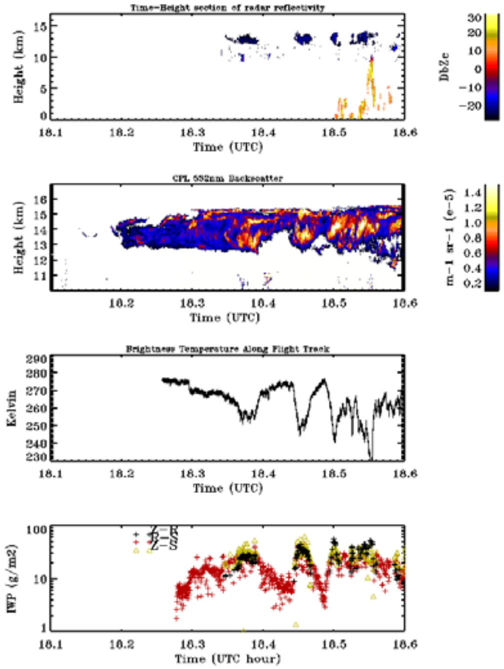

Figure 4. (a)southbound leg, CRS, Cloud Profiling Lidar (CPL; data provided courtesy Matt McGill),T_b, and retrieved *IWC*.

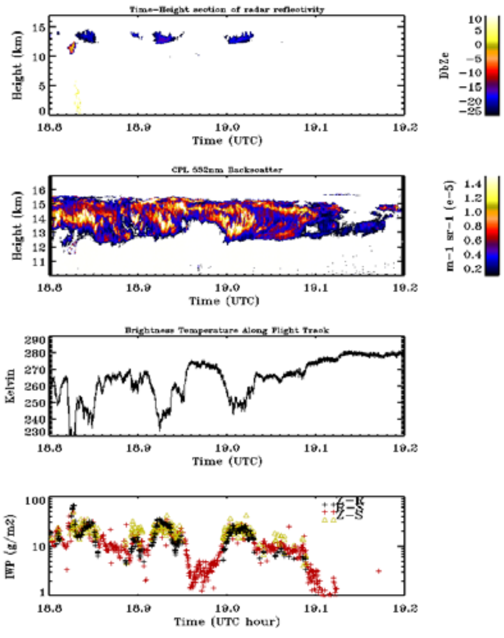

Figure 4. (b)northbound leg, CRS,CPL,T_b, and retrieved *IWC*.

Cirrus layers often have a vertical structure where the layer tops are optically tenuous and composed of small particles with larger particles and higher water contents in the lower portions of the layer (Mace et al., 1997). Cloud radars are known to often not sense the full vertical extent of cirrus layers due to this characteristic structure (Sassen and Mace, 2002). We find such a structure in the tropical cirrus observed on 26 July. Since the ZR algorithm requires the layer-averaged value of *Z* (i.e. $\overline{Z} = \frac{\sum_{base}^{top} Z(h)}{\Delta h}$ where *h* denotes height and Δ*h* denotes the layer thickness), using the radar to estimate Δ*h* results in systematic biases in the derived cloud properties. Since $\sum_{base}^{top} Z(h)$ is not greatly biased by not sensing the very low values of *Z* near cloud top, the error arises due to an incorrect value of Δ*h* that results in values of $\overline{Z}$ and β_a that are too large. Therefore, when the radar-detected cloud top is lower than the lidar-detected cloud top, the lidar-detected cloud top and the radar-detected cloud base are used to specify the layer thickness in the ZR and ZS algorithms. Specifying the layer thickness in this way will improve the retrieval accuracy overall, because the radar reflectivity factors below the detection of the radar do not contribute much to $\sum_{base}^{top} Z(h)$. In practice when the radar-detected cloud thickness is less than 30% of the lidar-detected cloud thickness, the above replacement is not employed since the total value of the radar reflectivity factor for the undetected layer may be equivalent to the total value of that for the detected layer. The three algorithms are consistent within the estimated 30% uncertainties.

On 29 July 2002, there was light maritime cirrus off the east coast of Florida in the early afternoon, and a significant thunderstorm that developed north of Naples around 1730 UTC that produced an extensive cloud deck moving northwestward off the Florida coast during the afternoon. The ER-2 flew a N-S traverse along the Florida west coast and then back to Key West over the water. The ER2 then headed off the east Florida coast and to the Bahamas. Several legs were then flown across the east and west ground sites, and then some E-W legs north of the ground sites, flying over the thunderstorm activity in the Naples area.

The retrievals are depicted in Figure 5. Cirrus clouds are broken in this case, and the cirrus properties are quite variable. The properties of the thick cirrus are retrieved from the two radar-involved algorithms, and those of the thin cirrus occurring around 16:03:00 UTC, which are below the detection threshold of the CRS, are retrieved from the RS algorithm. The two radar-involved retrievals agree well for cirrus during time the period from 15:48:00 to 15:54:00 UTC, but demonstrate some scatter for the other two thick cirrus periods around 16:18:00 UTC and 16:33:00 UTC. The retrievals from the ZR algorithm vary with time due to the wide range of the cloud layer emittance, since the brightness temperature observed from the MAS vary substantially, and the difference perhaps comes from a mismatch between the spatial registration of the measurements. A high correlation (0.8) between the IWPs retrieved from the ZS algorithm and those retrieved from the ZR algorithm for the whole time period is shown in Figure 6.

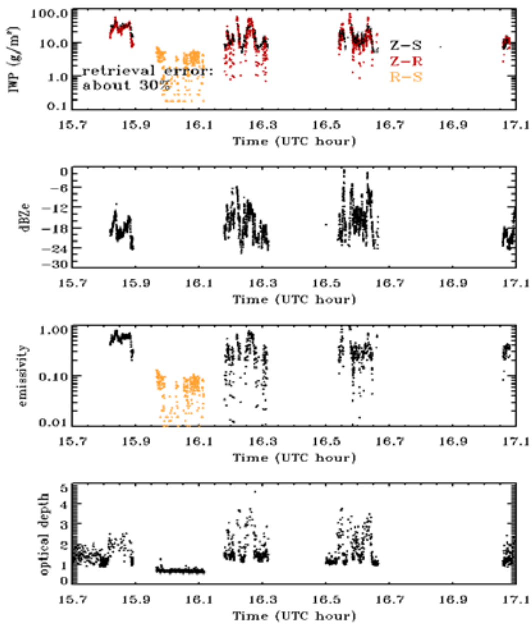

Figure 5. (a) Retrieved *IWP* (b) layer-averaged radar reflectivity (c) cloud layer emissivity derived from MAS observations (d) optical depth.

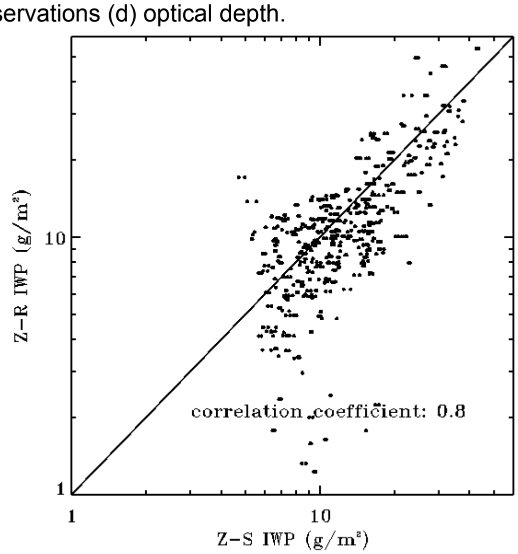

Figure 6. Correlation between IWP retrieved from ZR and those retrieved from ZS for the time period from 15.7 to 17.1 UTC.

An algorithm using ground based radar reflectivity and interferometer data (Mace et al. 2005a) has been developed and applied extensively to ARM observations (Mace et al., 2001, Mace et al., 2005b). This algorithm (hereafter referred to as the A-ZR algorithm) has been validated using aircraft data and now has reasonably well-known error characteristics as discussed in Mace et al. (2005a) where they show that the uncertainty in r_e and IWP are on the order of 30% and 20% respectively with negligible bias. The A-ZR results are appropriate for comparison with the algorithms proposed above for the A-Train.

To make this comparison as realistic as possible, MODIS data are combined with the MMCR and the MPL data from the ARM SGP site during the overpass instant to derive cloud properties. A 15 km × 15 km region centered on the ARM SGP site from the MODIS granule is selected, and the pixels with 1 km resolution in this region are considered. Since the typical wind velocity at cirrus levels is about 25 m/s, the radar reflectivity factor and the lidar-derived transmissivity are averaged for 10 minutes to combine with MODIS data for retrieving cirrus microphysical properties. The results are shown in Figure 7 (a), (b), and (c) derived from the MODIS overpasses of the SGP site. The correlation coefficients are similar for the three algorithms, and larger than 0.9. The slope for the ZR algorithm is slightly larger than 1, while those for the ZS and RS algorithms are slightly smaller than 1. The bias is relatively small, and the differences come from the fact that the effective density (Brown and Francis, 1995) in the A-ZR algorithm is a different treatment for ice crystals than the empirical constants in the A-Train algorithms. The comparisons show good overall agreement.

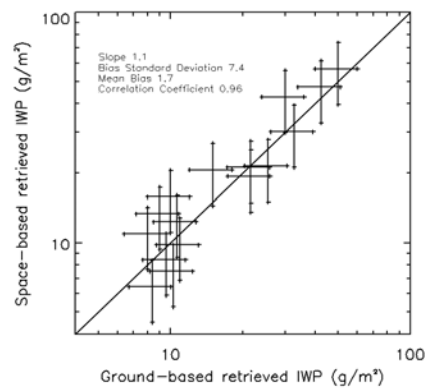

Figure 7 (a). Comparison between the ground-based retrieval and the ZR algorithm.

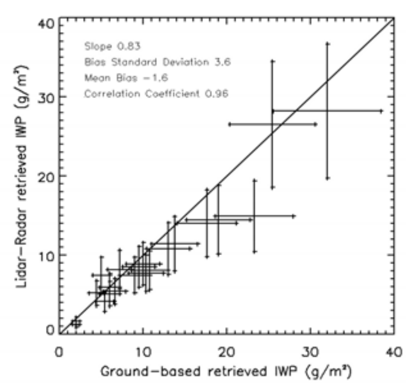

Figure 7 (b). Comparison between the ground-based retrieval and the ZS algorithm.

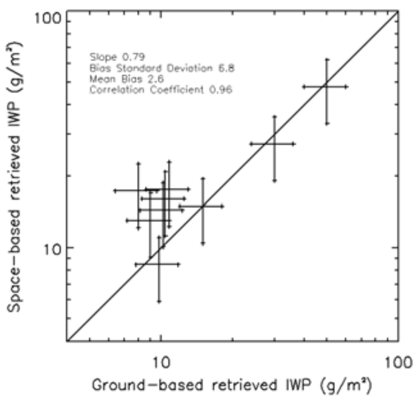

Figure 7 (c). Comparison between the ground-based retrieval and the RS algorithm.

5. Summary

A suite of algorithms, referred as the ZR, ZS, and RS algorithms, for retrieving ice cloud microphysical properties from multiple remote sensors have been developed for measurements from the A-Train. The suite of algorithms exploit the synergy of the active and passive measurements to treat a wide range of cirrus situations ranging from optically tenuous cirrus in the tropopause transition layer in the tropics to thicker cirrus that populate up to 30% of the global troposphere. Operational implementation of these algorithms to A-Train data will provide the opportunity to significantly extend our present understanding of cirrus cloud properties.

The sensitivity of the two radar-involved algorithms to the input data reveals that the retrieved *IWPs* depend to a nearly equal degree on the observations. But the RS algorithm is the most unstable among the three due to the second moment dependence of the observations on the size distribution. The retrieval parameters are also sensitive to the empirical constants describing the relationships between the ice crystal maximum dimension and the ice crystal area and mass assumed in the algorithms. This sensitivity leads to large uncertainties since the empirical relationships are not well documented on a global scale although work on the available in situ data is continuing (Heysmfield et al. 2004).

The suite of algorithms is implemented using data collected during CRYSTAL-FACE mission in July 2002 where the NASA ER2 was instrumented with a suite of instruments similar to the A-Train. The three algorithms are consistent within the estimated uncertainties for the first case study, and there is a high correlation (0.8) between the two radar-involved algorithms for the second study. The three algorithms are evaluated with the A-ZR algorithm separately, and a good linear relationship between the validated A-ZR algorithm and the suite of the algorithms is found with correlation coefficients around 0.96. There are also reasonable small bias standard deviations for the three algorithms.

6. Reference

Aydin, Kultegin and Thomas M. Walsh, 1999: Millimeter wave scattering from spatial and planar bullet rosettes. IEEE Transactions on Geoscience and Remote Sensing, 37, 1138-1150.

Dowling, D. R., and L. F. Radke, A summary of the physical properties of cirrus clouds, *J. Appl. Meteorol.*, 29, 970-978, 1990.

Heymsfield, Andrew J. and Jean Iaquinta, 2000: Cirrus crystal terminal velocities. J. Atmos. Sci., 57, 916-942.

Heymsfield, Andrew J., et al., 2002: Observations and parameterizations of particle size distributions in deep tropical cirrus and stratiform precipitating clouds: results from in situ observations in TRMM field campaigns. *J. Atmos. Sci.*, **59**, 3457-3491.

Liou, K. N., 2002: an introduction to atmospheric radiation. *Academic Press.*

Mace, G. G., T. P. Ackerman, and E. E. Clothiaux, 1997: A study of composite cirrus morphology using data from a 94-GHz radar and correlations with temperature and large-scale vertical motion. *J. Geo. Res.*, 102(D12), 13,581-13,593.

Mace, G. G., E. E. Clothiaux, and T. A. Ackerman, 2001: The composite characteristics of cirrus clouds: bulk properties revealed by one year of continuous cloud radar data. *J. Climate*, 14, 2185-2203.

Mace, G, G, 2002: On retrieving the microphysical properties of cirrus clouds using the moments of the millimeterwavelength Doppler spectrum. *J. Geophys. Res*. **107**, 4815-4831.

Mace(a), G. G., Y. Zhang, S. Platnick, M. D. King, P. Minnis, and P. Yang, 2005: J. Appl. Meteoro., 44, 221-240.

Mitchell, D. L., 1996: Use of Mass- and Area-Dimensional Power Laws for determining precipitation particle terminal velocities. *J. Atmos. Sci.*, 53, 1710-1723.

Stephens, G. L., et al., 2002: The CloudSat mission and the A-Train. Bull. Am. Meteorol. Soc., 83, 1771-1790.

Wylie, D.P., and W.P. Menzel, 1989: Two years of cloud cover statistics using VAS. *J. Climate Appl. Meteor.*, **2**, 380-392.

Wylie, D.P., Menzel, W.P., Woolf, H.M., and Strabala, K.I., 1994: Four years of global cirrus cloud statistics using HIRS. *J. Climate*, **7**, 1972-1986.

Yang, Ping, M. G. Mlynczak, H.L. Wei, D. P. Kratz, B,A. Baum , Y. X. Hu, W. J. Wiscombe, A. Heidinger, and M. I. Mishchenko, 2003: Spectral signature of cirrus clouds in the far-infrared region: single-scattering calculation and radiative sensitivity study. *J. Geophys. Res.*, 7019-7031.